SNAME102 Autonomous Robotic Boat 2013 Competition

Advisor: Professor Yung-Yu Chen

Li-Pang Huang, Chia-Chuan Ku, Pai-Hsun Lee,
Chao-Wei Chen, Ka-Yin Li, Li-Yu Huang,
Yi-Hsiu Lee, Nian-Ting Yang, Ting-Wei Chen,
Yu-Ching Lin, Pei-Yu Chang, Wei-Min Hu

Department of System and Naval Mechatronics

Engineering, National Cheng Kung University, Taiwan

Abstract

SNAME 102, designed by NCKU Roboboat Team, is on the purpose of achievement of AUVSI Foundation and ONR's 6th International Roboboat Competition. It is the 4th generation from the prototype SNAME 99.

In the design part, we redesign the twin hull of SNAME 101 into a trimaran to gain buoyancy and enlarge the deck area. Moreover, it will enhance the capability of straight sailing. In programming, we not only challenge new missions, but endeavor to better the capacity of "Navigate the channel", the mission we failed last year.

1. Introduction

SNAME 102 Robotic boat, developed for the 5th Annual International Roboboat Competition, is even more improved and maneuverable than SNAME 101. After analyzing pros and cons of SNAME 101, we transform it into the trimaran. The new design becomes much more longer in length overall, which means the maneuverability is polished, and the total buoyancy of SNAME 102 is lot more than the previous generation as well. With the advanced mechanical systems and better sensors including cameras, compass, GPS, and IR sensor, SNAME 102 is able to complete the challenge. The roboboat has been fully tested and regulated for several months.

2. Mechanical System

2.1 Ship Design

Based on SNAME 101's twin hull ship of last year, a multihull design concept is still used in this year due to easy transportation and the dimension limitation of the flight package regulation. However, because of some lessons learned from last year, we refined the notion of the ship.

First, SNAME 101's deficiency of buoyancy

which means the deck might be too close to the water surface and that will endanger the electronic devices. Hence, we transform SNAME 102 into trimaran which can provide required displacement and enough freeboard.

Second, the larger the side projected area is, the straighter the ship will sail. On account of SNAME 101 can not sail very straightly, we stretch the length overall (Loa) of SNAME 102 by protruding the central hull. Therefore, we increased the maneuverability of SNAME 102.

Third, in order to keep the yawing maneuverability and lessen the initial trim, we set the propeller forward to the preposition nearing mid-ship.

Therefore, the advantages of the trimaran are as follows:

- Easy transportation: The ship can be disassembled into three single hulls and fabricated easily.
- Large platform for installing multipurpose equipment.
- Deeper freeboard prevents the electronic devices from water.
- Perfect maneuverability includes both straight sailing and circling.
- A pair of outboard motors are used instead of a rudder.
- Large transverse stability.

2.1.1 Initial Design

i. Designing Condition

- The trimaran is designed under the condition as the follows.
- Speed (Vs):

We approximately calculate the speed of ship that can support us finishing all missions and going back to the dock in 20 minutes. The ship speed, Vs , should be at least **2knots**.

- Dead Weight(DW):

Estimation of the loading weight is given in table 2-1.

Dead weight	Value	Unit
Propeller*2	5	kg
Computer	3	kg
Shooter	3	kg
Robot Arm	3	kg
Camera	2	kg
Dead Weight	16	kg
Dead Wieght+Margin (10%)	17.6	kg

Table 2-1: Estimation of Dead weight

ii. Principle Dimension

The principal dimension of the trimaran is designed due to the dimension limitation of the flight package regulation. The limitations of China Airline and American Airline are as follows.

- China Airline:

Length + Width + Height ≤158 cm and Weight≤23 kg.

- American Airline:

Length + Width + Height ≤158 cm and Weight≤23 kg.

Central Body	Value	Unit
Length	1	m
Breadth	0.15	m
Draft	0.2	m
Free Board	0.05	m
Side Body	Value	Unit
Length	1	m
Breadth	0.15	m
Draft	0.2	m
Freeboard	0.05	m

Table 2-2: Principal Dimension of each body

iii. Displacement

In the beginning, we set Cb value as 0.5, the general value of high speed vessel. Then, we can estimate the displacement and make sure whether the buoyancy is enough for the dead weight or not.

Light Weight	Value	Unit
Hull	17.7	kg
Deck	3.83	kg
Connecting Structure	2	kg
Light weight	23.53	kg
Light weight + margin (10%)	25.83	kg

Table 2-3: Estimation of Light weight

Displacement	Value	Unit
Trimaran	45	kg
Trimaran – Light weight	19.17	kg
Dead weight	17.6	kg

Table 2-4: Estimation of Displacement

Therefore, we can understand the buoyancy is enough for the dead weight.

2.1.2 Final Design

Initially, we use Rhino4.0 to generate the lines. Next, we use Orca 3D to analyze its hydrostatics property. Finally, according to the ITTC formula, we can estimate the ship resistance and required power.

We made some assumptions as below:

a. Neglect the residual resistance.

b. Wake coefficient = 0.5

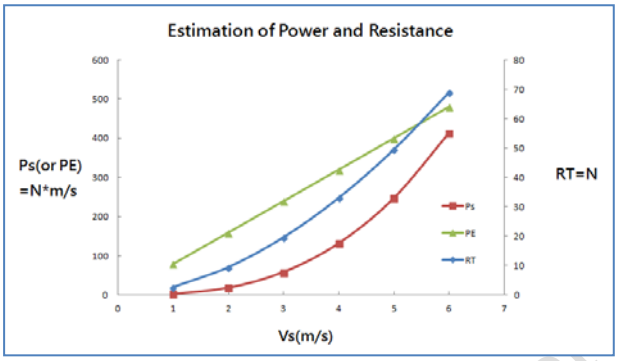

Fig. 2.1 Estimation of Power and Resistance (Ps = Power of Ship, PE= Power of Propeller, RT= Resistance of Trimaran)

Trimaran	Value	Unit
Length of over all	1.2	m
Extreme Breadth	0.75	m
Depth of ship	0.25	m
Design Draft	0.2	m
Freeboard	0.05	m
L/B	1.6	m
Displacement	47.52	kg
Wet Area	1.14	m^2

Table 2-5: Final Dimension of the designed Trimaran

2.2 Fabrication Of Ship Body

After using Rhinoceros 4.0 platform to build the 3D model (Fig. 2.2), Aran Chen, tooling center assist advisor of Horizon Yacht, help us with fabrication. Each hull was made of 6 layers of 100cm x 50cm x 5cm high-density foam plates, glued together with AB composite glues.

With their sophisticated craftsmanship and advanced 5-axis CNC machine, the shape of ship hull is perfectly modeled. After the hull is complete, the ship is coated with a layer of white waterproof paint.

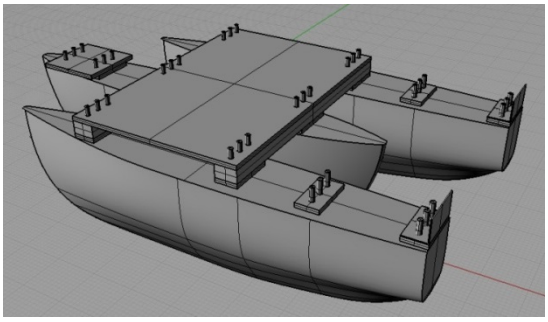

Fig. 2.2 3D Trimaran Model

2.3 Propulsion

A pair of motors, 36 pounds thrust in maximum in each, are dangled from the stiffener of stern. Not only do they provide excellent maneuverability, but they also make us control the ship without the rudder.

An outboard thruster provides nearly 18 lbs (8.16 kg) when an 180W of power is supplied.

Fig. 2.3 Outboard motor

2.4 The Shooter

2.4.1 Mechanical Part

The basic structure concept of the shooter is from the M40 recoilless rifle. In order to accomplish the mission, three important ideas must be included in the design. The first one is adjustable direction. We put two servomotors in the shooter. One can change horizontal direction while the other makes the angle of firing. The second is the reloading system. With the reloading system, we will have chance to adjust the right angle. Next, we designed an exquisite gadget to prevent reloading from jam. Finally, we use a cylinder to keep high pressure gas, and an electronic valve as the switch.

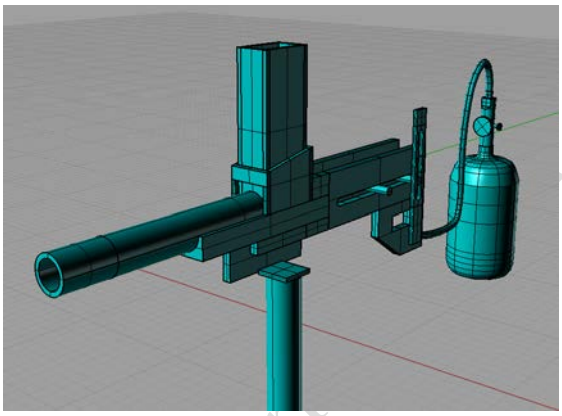

Fig. 2.4 Mechanical design of Shooting through the hoop

The mission is shoot bullets into the hoop with 2 feet diameter. According to the rule of this competition, there are two limits. One is that the bullet must be entirely made of foam, and the other is that it must be shot using compressed air.

The former is easily attainable by using Styrofoam and we only consider what to do to let the bullet fly smoothly. After the testing, we decide to shape Styrofoam becoming cylinder rather than pellet.

The latter is much more complex. SNAME 102 must have the ability to store pressured air by itself. Consequently, we choose the steel cylinder to load the high pressure air.

A crucial point is that we are from Taiwan, and all the equipment must be carried by the airplane, but the high pressure bottle is forbidden on the plane. Therefore, we will bring an empty cylinder which could reload high pressure air with an air compressor. Besides, the air compressor shown in Fig. 2.5 must provide the pressure in the range 7 bars to 10 bars so that we can make sure we have enough power to

reload.

Fig. 2.5 Air compressor and high pressure bottle

Furthermore, if we want to supply the stability of the pressure, the pressure regulating valve is necessary. It will keep the pressure identical while each shooting. After several trials, we figure out that the pressure in at least 6 bars would shoot the bullet approximately three meters away. That is the most suitable range for shooting hoops.

Fig. 2.6

If the shooter fires with higher degrees of the elevation, it is more difficult to shoot into the hoop. Because of the parabola path, it will vertically fall down to the ground. After the experiments, a 20 degree of the elevation angle is applicable. Consequently, the bullet will be easily controlled flying in the level path.

When we prepare to fire, a 5V signal will be sent by the computer to the relay. Then the electrical valve will be switched on. When the valve is on, it releases high pressure air to push the bullet to out of the shooter. After firing, the shooter will reload the bullet for the next fire.

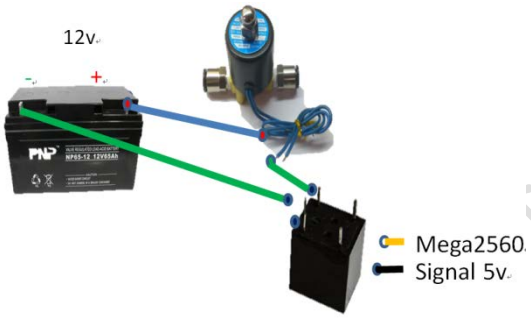

Fig. 2.7

Fig. 2.8

2.4.2 Image Processing of The Shooter

The image processing plays an important role in the above mission. Three primary steps are included in the algorithm for achieving this mission. The first step of the mission is to find the right heading direction where the camera can identify the hoop by the electrical compass. Next, SNAME 102 can automatically calculate the right direction to approach the location which is in front of the hoop (Fig2.9). The second step is image processing. When the camera detects some red objects, the message will be sent to compare with the predefined

template which consists of the images of the hoops. Once the image of hoops is identified matching the template, SNAME 102 will define it as a qualified target and starts to track it. The final step is missile firing. Once the radius of the circle image is larger than the setting value, SNAME102 will stop and give a signal to execute the firing mission.

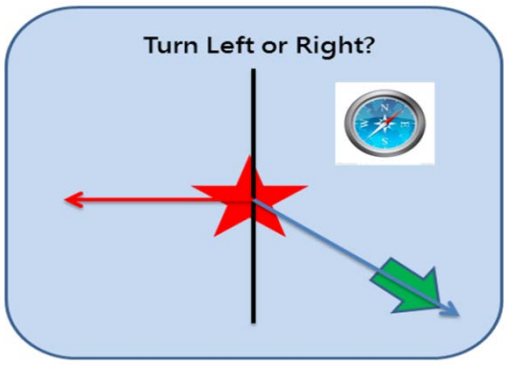

Fig.2.9 Navigation of electronic compass

2.5 The Arm

In order to challenge "Capture the flag", we build a robotic mechanical arm with five servomotors is developed. First, we drew the design chart (Fig. 2.10) and imaged that it is directly by using two servomotors to control the arm. After building it and several tests, we found out it was infeasible. At last, we made out a five servomotors mechanical arm (Fig. 2.11) and it can perfectly make a series of catch a flag action.

By using Webcam and LabVIEW, we can capture the image and calculate the exactly location of the flag. If the location of the flag is in the reachable area, the arm will be turned on, and controlled by the program to catch the object.

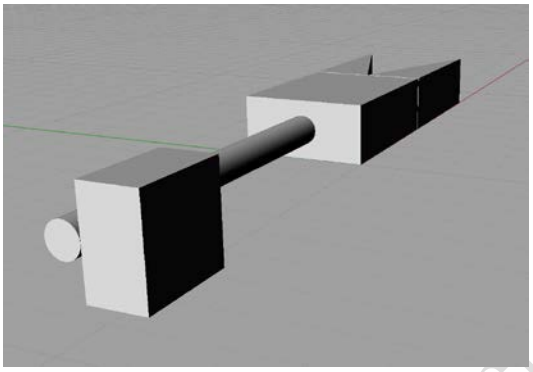

Fig.2.10 The Premier Design Chart

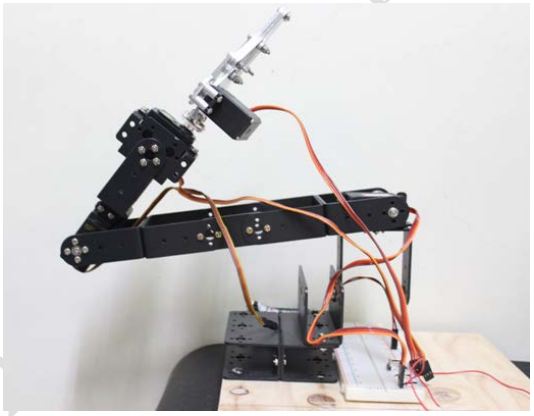

Fig.2.11 The Arm

3. Electrical Design

GIGABYTE GA-H77M-D3H main board with INTEL CORE i5 3470 CPU is utilized to be the major control unit for this boat robot and the usage of TRANSCEND JM1333KLN-4G memory, is to increase the responses of feedback signals that includes as: GPS, Camera and Compass, where communications between NEMA of GPS and heading angle of the used Compass and the controlled main board are translated by UART Protocol to USB. In this investigation, control commands for guiding the boat robot are performed by the following steps: 1. Heading angle calculated by software LabVIEW first and then, 2. The feedback linearization based control in (16) is discretized and translated with UART Protocol to Micro controller: Arduino-Mega2560 and a series of PWM signals drives DC motors to generate

torques to rotate propellers. Besides, micro controller: Arduino- Mega2560 is also adopted to control apparatuses in the boat robot as the servo motor of robot arm, and magnetic switch of shunting machine, and so on.

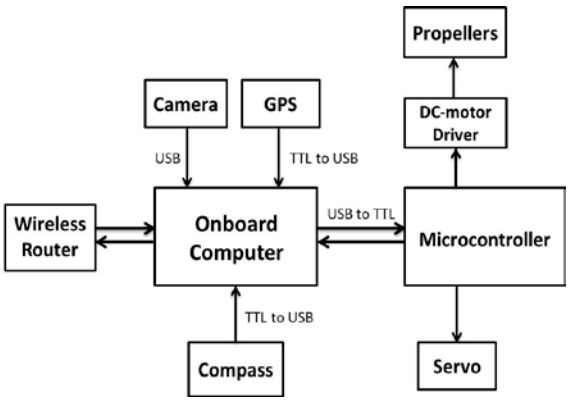

Fig.3.1 Electrical System

4. Power System

For the purpose of saving the space and increasing the usage duration, a lithium ion battery with type number: AMP20 Lithium Ion Prismatic Cell can steadily offer a nominal voltage: 3.3V and nominal capacity: 20Ah is taken into consideration based on the excellent advantages: high power and flimsy proof. By serial connecting 4 pieces of the above battery, a total voltage 13.2 can be realized to supply the boat robot with a full payload for running over one working hour.

Adjustable voltage regulars that are on the shelf and cheap generally are utilized to offer stable voltages for the main board with 12V and wireless router with 9V, and the advantage of this design is: adjustable voltage regulators can eliminate the sudden high voltage peaks or a huge of decrease in supplied voltage and avoid the preventable shut-down of the power system of boat robot as operation modes of propellers suddenly changes which always needs large power immediately to achieve the mission, and this behavior will result in a shut-down of the overall boat robot system in practical design. This power management module overcomes those two problems and steadily and continuously offers voltages to the whole system.

As to the thruster control design, a DC motor driver which can be precisely controlled to be a switch or average the input voltage with PWM Pulse is selected for the purpose of rotating propeller counterclockwise or clockwise.

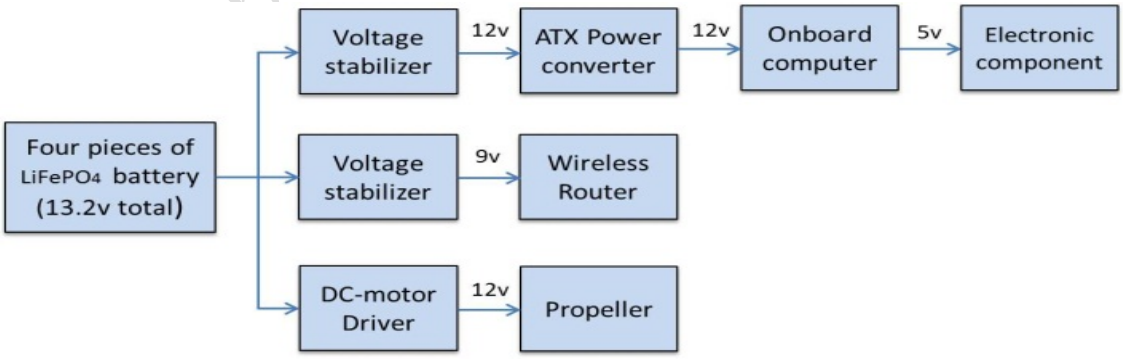

Fig.4.1 Parse tree diagram of power system

5. GPS Module

5.1 GPS Module

In the cause of accurate orientation, we add Fastrax UP501 Antenna GPS module to our sensory system. Fastrax UP501 GPS receiver module with embedded GPS antenna enables high performance navigation in the most stringent applications and solid fix even in harsh GPS visibility environments.

5.2 Research Procedures

5.2.1 Control Law Design Of Unmanned Surface Vessels

In this investigation, guidance law design of autonomous unmanned surface vessel design is divided into two parts. The first part is the tracking design of desired predefined waypoints.

As shows in Figure 5.1, designers predefined a set of waypoints that will be tracked are given as, and the real-time vessel's positions are assumed to be measured by an embedded GPS. Based on these two messages, the real-time tracking error can be calculated until the tracking mission achieved.

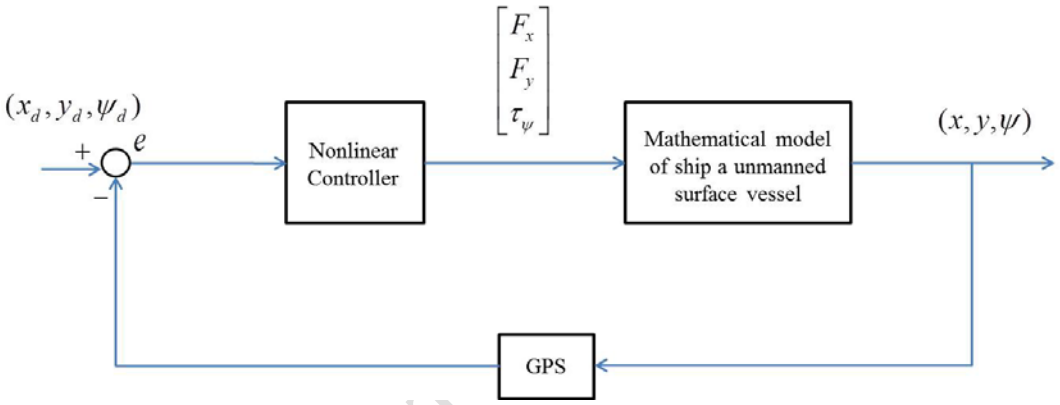

Fig. 5.1 Control flow chart of the unmanned surface vessel

5.2.2 Mathematical model of the unmanned surface vessel

General speaking, equation of motion of surface vessels are always expressed by a 3 DOF (degree of freedom) mathematical model. The body frame coordinate and earth frame coordinate of an unmanned surface vessel is illustrated as Figure 5.2.

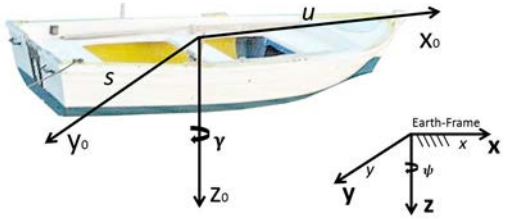

Fig. 5.2 Illustration of body frame and earth frame of the unmanned surface vessel

By choosing system state variables as: $v=[u \quad s \quad r]^T$ is defined as the vector of linear velocity and angular velocity of vessels in body frame , $\eta=[x \quad y \quad \psi]^T$ is the position and heading angle of the controlled unmanned surface

vessels in the earth frame, and $\tau=\begin{bmatrix}F_x & F_y & \tau_\Psi\end{bmatrix}$ is the control force and torque acted in surface vessels, respectively. Based on the above definition and Lagrangian approach, dynamics of the controlled unmanned surface vessel can be expressed in body frame as:

$$M\dot{v}+C(v)v=\tau \tag{1}$$

M: Inertia matrix;

$C(v)$: Coriolis force;

τ: Control input;

Where the parameter matrices of system model of the controlled surface vessel can be further parameterized as:

I. Inertial matrix of the controlled unmanned surface vessel:

$$M=\begin{bmatrix} m & 0 & 0 \\ 0 & m & mX_G \\ 0 & mX_G & I_z \end{bmatrix} \tag{2}$$

Where

X_G: Distance from gravity center to x axis

I_Z: Moment of inertia with respect to z axis

m: Weight of the unmanned surface vessel

And M possesses the following property:

$$M=M^T>0$$

II. Parameterization of Coriolis force and central force matrix.

$$C(v)=\begin{bmatrix} 0 & 0 & -ms-mX_Gr \\ 0 & 0 & m \\ ms+mX_Gr & -m & 0 \end{bmatrix} \tag{3}$$

And $C(v)$ has the following property.

$$C(v)=-C^T(v)$$

The above vessel's model is described by body frame, and for practical design purpose, this model should be then transformed into earth frame. The kinematic relationship between body frame and earth frame of the unmanned surface vessel can be introduced by the following equation:

$$\dot{\eta}=J(\eta)v \tag{4}$$

Earth-fixed Vector Representation: Based on the transformation equation $J(\eta)$, surface vessel's coordinate will be transformed into earth coordinate by a relationship as:

$$\dot{\eta}=J(\eta)v \Leftrightarrow v=J^{-1}(\eta)\dot{\eta} \tag{5}$$

Where

$$J(\eta)=\begin{bmatrix} \mathrm{c}\psi & -\mathrm{s}\psi & 0 \\ \mathrm{s}\psi & \mathrm{c}\psi & 0 \\ 0 & 0 & 1 \end{bmatrix} \tag{6}$$

$s\cdot=\sin(\cdot)$; $\mathrm{c}\cdot=\cos(\cdot)$

By the definitions in (4) and (5), we have

$$\ddot{\eta}=J(\eta)\dot{v}+\dot{J}(\eta)v \tag{7}$$

Then

$$\dot{v}=J^{-1}(\eta)[\ddot{\eta}-\dot{J}(\eta)J^{-1}(\eta)\dot{\eta}] \tag{8}$$

The controlled dynamics in earth frame coordinate of the unmanned surface vehicle is then represented by a formulation as:

$$M_\eta(\eta)=J^{-T}(\eta)MJ^{-1}(\eta) \tag{9}$$

$$=\begin{bmatrix} m_{11}c\psi^2+m_{22}s\psi^2 & m_{11}c\psi s\psi-m_{22}c\psi s\psi & -m_{23}s\psi \\ m_{11}c\psi s\psi-m_{22}c\psi s\psi & m_{22}c\psi^2+m_{11}s\psi^2 & m_{23}c\psi \\ -m_{23}s\psi & m_{23}c\psi & m_{33} \end{bmatrix}$$

And $m_{11}=m$, $m_{22}=m$, $m_{33}=I_z$ and $m_{23}=m_{32}=mX_G$. X_G is the center of gravity of the unmanned surface vessel. Besides, the transformed Coriolis force can be further described as follows:

$$C_\eta(v,\eta)=J^{-T}(\eta)[C(v)-MJ^{-1}(\eta)\dot{J}(\eta)]J^{-1}(\eta)$$

$$=\begin{bmatrix} a_{11} & a_{12} & a_{13} \\ a_{21} & a_{22} & a_{23} \\ a_{31} & a_{32} & a_{33} \end{bmatrix} \tag{10}$$

Where

$$a_{11} = -\dot{\psi} s\psi c\psi (m_{11} - m_{22})$$
$$a_{12} = \dot{\psi}(m_{11} - m_{11} s\psi^2 + m_{22} s\psi^2)$$
$$a_{13} = c_{13} c\psi - c_{23} s\psi$$
$$c_{13} = -c_{31} = -ms - mX_G r$$

And

$$c_{23} = -c_{32} = mu$$
$$a_{21} = \dot{\psi} m_{11} c\psi^2 - \dot{\psi} m_{11} - \dot{\psi} m_{22} c\psi^2$$
$$a_{22} = \dot{\psi} s\psi c\psi (m_{11} - m_{22})$$
$$a_{23} = c_{23} c\psi + c_{13} s\psi$$
$$a_{31} = c_{23} s\psi - c_{13}\, c\psi - \dot{\psi} m_{23} c\psi$$
$$a_{32} = -c_{23} c\psi - c_{13} s\psi - \dot{\psi} m_{23} s\psi$$
$$a_{33} = c_{33}, \text{ and } \; c_{33} = 0$$

Based on the above arrangements, an equation of motion for an unmanned surface vessel will be expressed in earth frame as:

$$M_\eta(\eta)\ddot{\eta} + C_\eta(\nu,\eta)\dot{\eta} = \tau_\eta \tag{11}$$

Where

$$\tau_\eta = \begin{bmatrix} F_x & F_y & T_z \end{bmatrix}^T$$

Define the tracking errors between controlled unmanned surface vessel and waypoints as:

$$\begin{aligned} e &= \eta - \eta_d \\ &= \begin{bmatrix} x \\ y \\ \psi \end{bmatrix} - \begin{bmatrix} x_d \\ y_d \\ \psi_d \end{bmatrix} \end{aligned} \tag{12}$$

Where it is the predefined position of desired waypoints and (i.e., it is at least twice differentiable) is the light-of-sight angle (LOS) between the unmanned surface vessel and waypoints. As the previous definition, it is the position and heading angle of the unmanned surface vessel.

Remark 1: *When* $\psi - \psi_d \to 0$*, it means unmanned surface vessel and the predefined waypoint in the head on condition. Therefore, the unmanned surface vessel will eventually hit the predefined waypoint if tracking error* e *is driven to zero before the unmanned surface vessel crosses the predefined waypoint.*

5.2.3 Design Objective

Consider system of the controlled unmanned surface vessel in (13). The design objective is mixed is to find a control law such that the following optimal performance can be achieved:

$$\min_{\tau_\eta(t)\in[0,t_f]} \left[e^T(t_f) e(t_f) \right] \tag{13}$$

For all $t_f \in [0,\infty]$

5.2.4 Control Law Design

For achieving the above design objective and guarantee the tracking performance, the easy-to-implemented feedback linearization method will be utilized and be mathematically derived in the following. Let us denote the system output as the tracking error e and τ_η is the control input; hence, we obtain the input-output relationship by the following mathematical derivations:

Step 1: Differentiate tracking error equation in (12) with respect to time, and then we have

$$\begin{aligned} \dot{e} &= \dot{\eta} - \dot{\eta}_d \\ &= J(\eta)\nu - \dot{\eta}_d \end{aligned} \tag{14}$$

From (14), it is obvious that no control messages τ_η can be found.

Step 2: Repeat the same mathematical operation as that in Step 1, then (14) becomes

$$\begin{aligned} \ddot{e} &= \ddot{\eta} - \ddot{\eta}_d \\ &= M_\eta(\eta)^{-1} \left\{ -C_\eta(\nu,\eta)\dot{\eta} + \tau_\eta \right\} - \ddot{\eta}_d \end{aligned} \tag{15}$$

Suppose $M_\eta(\eta)$ and $C_\eta(\nu,\eta)$ are exactly known, a feedback linearization control law can be represented in the following form

$$\tau_\eta = M_\eta(\eta) \left\{ M_\eta(\eta)^{-1} C_\eta(\nu,\eta)\dot{\eta} + \sigma \right\}$$

Where σ is given by $\sigma = [\sigma_1 \;\; \sigma_2 \;\; \sigma_3]^T$ and

$$\sigma_1 = \ddot{x}_d - \alpha_1(\dot{x} - \dot{x}_d) - \alpha_2(x - x_d) \quad (17a)$$

$$\sigma_2 = \ddot{y}_d - \alpha_3(\dot{y} \div y_d) - \alpha_4(y - y_d) \quad (17b)$$

$$\sigma_3 = \ddot{\psi}_d - \alpha_5(\dot{\psi} - \dot{\psi}_d) - \alpha_6(\psi - \psi_d) \quad (17c)$$

By substituting the control law (16) into (15), we get the following characteristic equation for tracking error dynamics of the closed-loop system as

$$\ddot{e} + A\dot{e} + Be = 0 \quad (18)$$

Where

$$A = \begin{bmatrix} \alpha_1 & 0 & 0 \\ 0 & \alpha_3 & 0 \\ 0 & 0 & \alpha_5 \end{bmatrix}, \quad B = \begin{bmatrix} \alpha_2 & 0 & 0 \\ 0 & \alpha_4 & 0 \\ 0 & 0 & \alpha_6 \end{bmatrix}$$

The coefficient $\alpha_i > 0$, for $i = 1,\ldots,6$ in (17) have to be selected so that the characteristic equation in (18) is a Hurwitz polynomial (i.e., roots of (18) are all in the left-half complex plane) and this implies that the overall system is asymptotically stable and tracking error e can be proven to converge to zero asymptotically with a convergence rate that depends on the choice of α_i

Simulation Result

The dynamical model parameters of the unmanned surface vessel have been given by Fossen [4], and the system parameters needed for simulation are listed as follows:

$$M = \begin{bmatrix} 25.8 & 0 & 0 \\ 0 & 33.8 & 1.0115 \\ 0 & 1.0115 & 2.76 \end{bmatrix}$$

And

$$C(\nu) = \begin{bmatrix} 0 & 0 & 33.8s - 1.0115r \\ 0 & 0 & 25.8 \\ -33.8s + 1.0115r & -25.8 & 0 \end{bmatrix}$$

The proposed control law is realized with

$$A = \begin{bmatrix} 1 & 0 & 0 \\ 0 & 1 & 0 \\ 0 & 0 & 1 \end{bmatrix}, \quad B = \begin{bmatrix} 1 & 0 & 0 \\ 0 & 1 & 0 \\ 0 & 0 & 1 \end{bmatrix}$$

For verifying the control performance of the proposed method to the unmanned surface vessel, two cases with predefined waypoints that are arbitrary chosen are given as below:

In this case, twelve predefined waypoints are given to test the tracking performance of this proposed method as following:

{(0,0) (0,160) (60,80) (120,150) (180,240) (260,150) (300,0) (346,-100) (250,-150) (150,-150) (90,-60) (0,0)}

Fig. 5.3 shows the course of the unmanned surface vessel with respect to waypoints in Case and the controlled unmanned surface vessel precisely approaches every predefined waypoint. The unmanned surface vessel's positions and heading angle tracking errors in Earth-fixed coordinate are shown as Figs. 5.4-5.6, and from these figs., the tracking errors are simultaneously convergent to zero asymptotically for each tracking period. Control commands included control forces in X-Y axis and control torque are shown as Figs. 5.7-5.9 for this simulation.

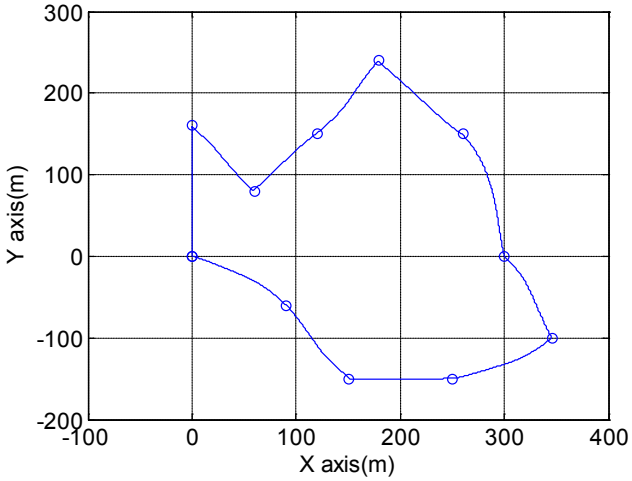

Fig. 5.3 Trajectory Plot

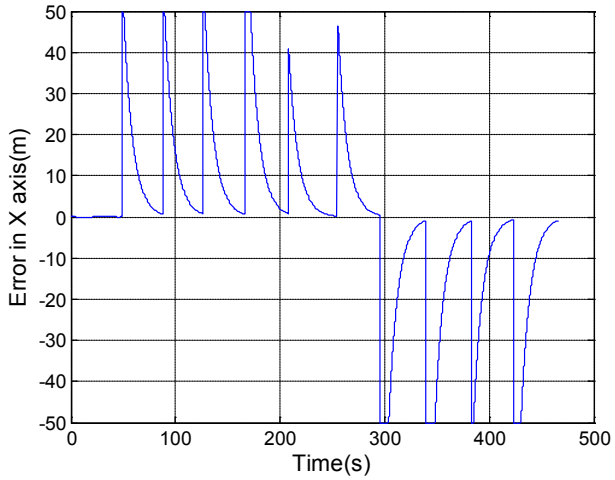

Fig. 5.4 Tracking error in X axis

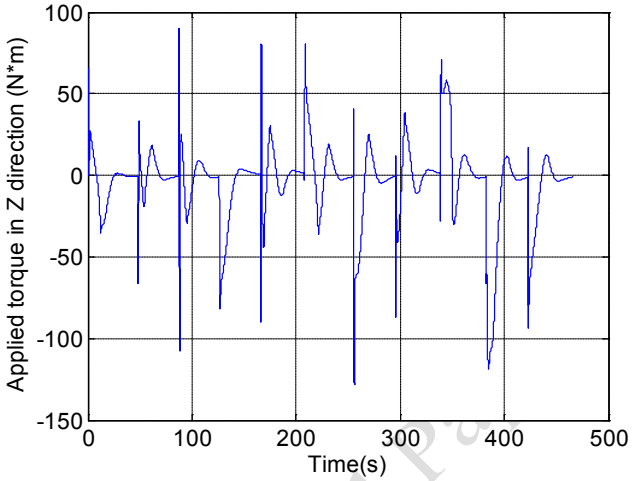

Fig. 5.7 Applied torque T_z

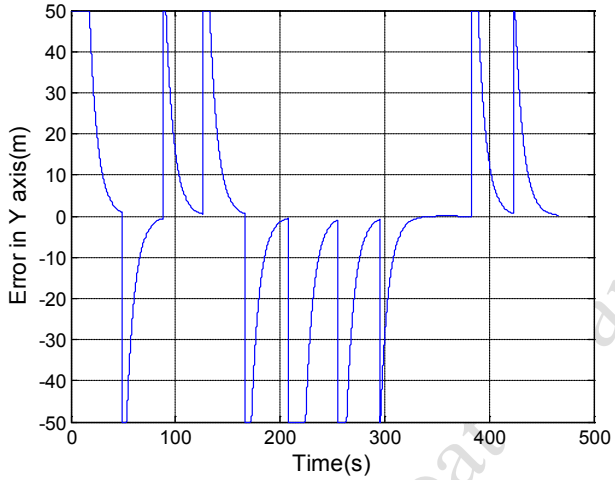

Fig. 5.5 Tracking error in Y axis

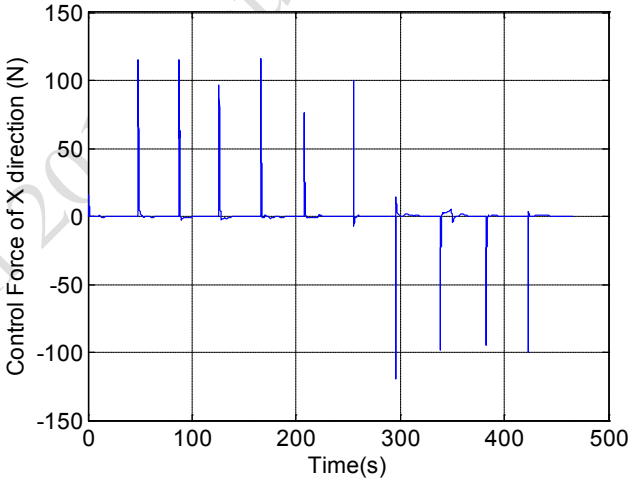

Fig. 5.8 Control history of *Fx*

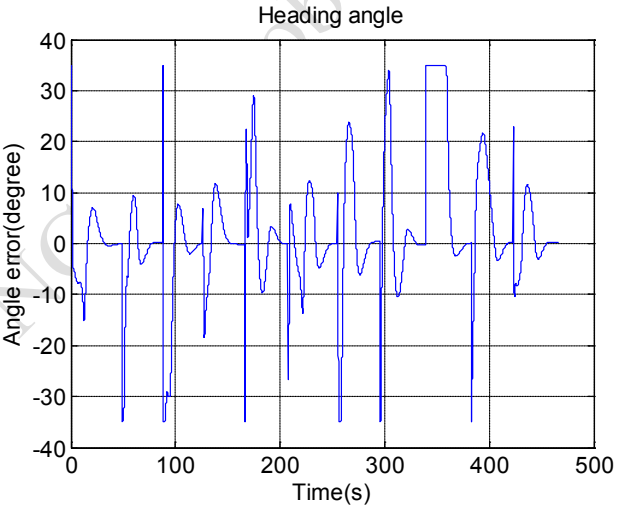

Fig. 5.6 History of heading angle error

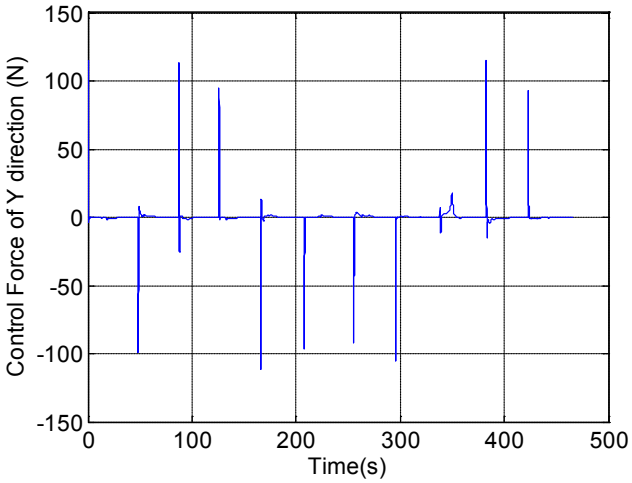

Fig. 5.9 Control history of *Fy*

6. Electrical Compass

In order to reach the standard of precise coordinates and less position error, we use the CMPS10 module. The CMPS10 module is a tilt compensated compass. Employing a 3-axis magnetometer and a 3-axis accelerometer and a powerful 16-bit processor, the CMPS10 has been designed to remove the errors caused by tilting of the PCB.

7. IR Sensor

7.1 Sensor

A type of IR sensor is S10 series with properties as followings:

(i) Output signal: 0~5V (linear) →matches format of Arduino.

(ii) Time response: 500ms

(iii) Ambient temp. : 0~60℃

(iv) Measurement temp.: 0~500℃

(v) Accuracy: ±1℃ or ±1.5℃

(vi) Distance-Spot ratio: 20:1

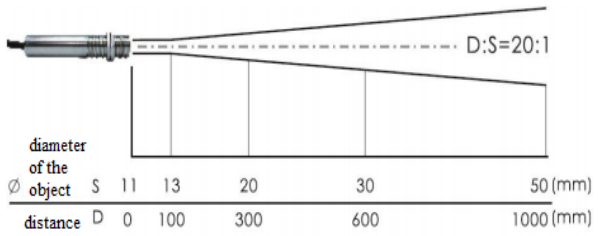

Fig. 7.1

7.2 Program Of IR Sensor

For the mission of hot objective detection, there are four plates with four pictures and one of them is at highest temperature (+20℃). To complete this mission, we need to compare each temperature of the plate and grab a name of the picture with highest temperature along with its GPS. It is necessary for SAME 102 to be equipped with a temperature sensor and a good image processing procedure as well, so we choose an IR sensor that can deal with measuring temperature in distance from the plates as well as program written by LabVIEW to handle a part of processing image through a computer and a webcam. The sensing structure of the IR system is shown as the following figure:

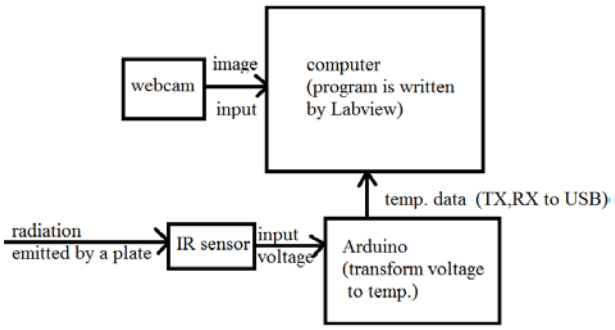

Fig. 7.2 Sensing Stricter of IR sensor

To deal with the captured images, we adopt LabVIEW as a programming software and LabVIEW Vision as the basic vision programming apparatus. LabVIEW Vision is applied for capturing image and filtering noise by tuning range of RGB, and then outputs the area, center of x and center of y of the objects. After these basic processing procedures, we utilize the output result to direct the boat robot, and compare each datum of temp. The elementary idea of the algorithm is given as below figure.

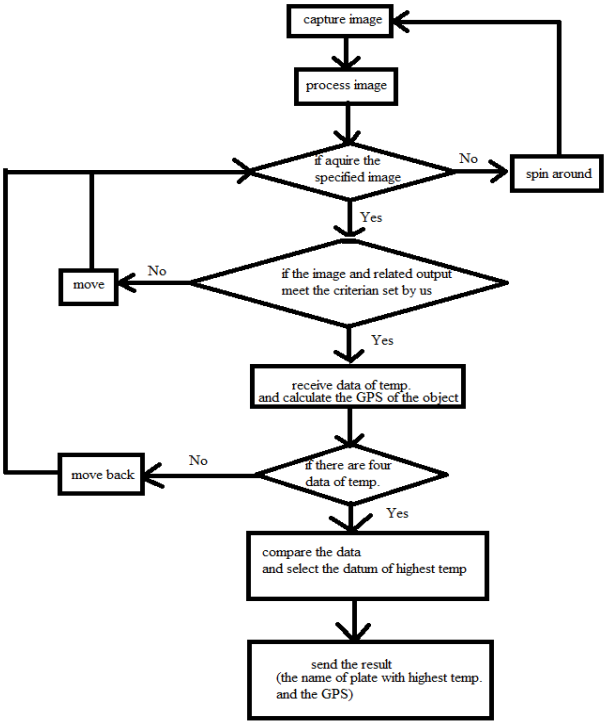

Fig. 7.3

When the computer receives the data of measured temperature, the distance between the plate and autonomous boat Robot can be denoted as D which should be in the range set up by the program. Therefore, we can calculate the horizontal location of the boat robot. The formula is

$$(x_p, y_p) = (x_b + D\sin\theta, y_b + D\cos\theta)$$

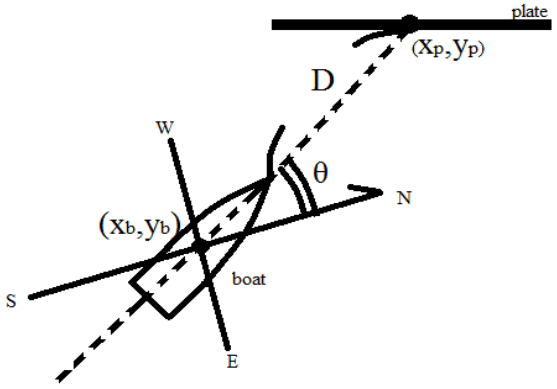

Fig. 7.4

The tough challenging of this mission is about processing image because we cannot alter luminance from source of sun and this factor would affect the result of processing image crucially.

8. Vision

8.1 Camera

USB cameras need little power to supply; it is very convenient settling in a system. It works if the batteries are full charged. By using USB cameras, SNAME 102 do not have to load extra weight and the camera can be set up anywhere on the vehicle.

Fig. 8.1 Logitech HD Webcam C525s

8.2 Image

At first, we can do image processing through LabVIEW Vision Assistant, which would display the outputs in every step, which let us properly select the target from background.

Selecting interest area is to reduce time to calculate image size and exclude unwanted region, so the process will be faster. The threshold is the simplest method of image segmentation by which one can filter noise roughly. Moreover, by the step of morphology mathematics, left noise will be eliminated and left some potential outputs to further detections, such as the geometric detection. After serial processes, computer will send commands to propeller system according to our algorithm.

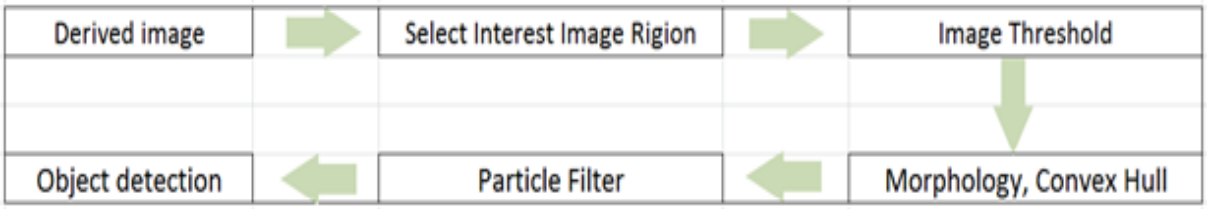

Fig. 8.2 Flow chart of image processing

9. Conclusion

Generally speaking, we inherit experiences from SNAME 101, vision programming especially. This year, we put great emphasis on designing ship, vision programming and autonomous control. In the hull part, we make a lot progress while assembling and delivering the ship. In the mission section, we have tried a lot navigating, capturing the flags, and shooting. The most important part is that we kept amending the code day and night. Though there are so many obstacles to the success, all of us tried to do our best and dedicated ourselves to better SNAME 102. After all, SNAME 102 will withstand the challenges.

We are grateful to the AUVSI Foundation for the chance to compete the competition. Also, we appreciate Horizon Yacht for the opportunity of building SNAME 102. Besides, we all feel an immense gratitude to our advisor, professor Yung-Yu Chen, who supports us and gives us encouraging words all the time. Finally, we learned the spirit of teamwork, and better ourselves through the competition.

10. Reference

[1] Davidson, K.S.M., and Schiff, L.I., "Turning and course keeping qualities of ships," *Trans. Soc. Nav. Archit. Mar. Eng.*, Vol. 54 (1946).

[2] Vukic, Z. "Improving fault handling in marine vehicle course-keeping systems," *IEEE Proc. Robotics and Automation Magazine*, Vol.6, Issue 2, pp. 39 – 52 (1999).

[3] Holzhuter, T., "LQG approach for the high precision track control of ships," *IEEE Proc. Control Theory Appl.*, Vol. 144, Issue 2, pp. 121–127 (1997).

[4] Fossen, *Guidance and Control of Ocean Vehicles*, John Wiley and Sons, New York, N.Y., pp. 19 (1994).